OPTIMIZED OXIDATIVE-ALKALINE TREATMENT OF AP1 RAMIE FIBERS FOR ENHANCED CELLULOSE PURITY AND TENSILE STRENGTH

DAM XUAN THANG,[*] NGO THUY VAN,[*] PHAM THI THU GIANG[*] and NGUYEN NGOC LINH[**]

[*]*Faculty of Chemical Technology, Hanoi University of Industry, Hanoi, Vietnam*
[**]*Faculty of Pharmacy, Thanh Do University, Hanoi, Vietnam*
✉ *Corresponding author: D. X. Thang, thangdx@haui.edu.vn*

Received April 10, 2025

In this study, an optimized oxidative–alkaline treatment was developed to improve the structural and mechanical performance of AP1 ramie fibers. A 7% calcium hydroxide [$Ca(OH)_2$] solution was employed in combination with oxidizing agents – hydrogen peroxide (H_2O_2), calcium hypochlorite ($Ca(OCl)_2$) and sodium hypochlorite (NaOCl) – to enhance delignification and hemicellulose removal. The treated fibers were characterized using Fourier-transform infrared spectroscopy (FTIR), scanning electron microscopy (SEM), tensile testing, colorimetric analysis and thermogravimetric analysis (TGA) to evaluate their physicochemical transformations. Among the tested conditions, the treatment with 4% H_2O_2 and 7% $Ca(OH)_2$ for 90 minutes yielded the highest performance enhancements, with tensile strength increasing by approximately 1.5 times – from 687.26 MPa (untreated) to 1061.60 MPa – and cellulose purity reaching 93%. Optimization of processing parameters using the Box–Behnken design and second-order regression modeling confirmed strong statistical significance ($R^2 > 0.99$) and model validation showed deviations below 5% between predicted and experimental values. These findings demonstrate the effectiveness of oxidative–alkaline processing for producing high-performance ramie fibers and the enhanced mechanical and structural properties of treated AP1 ramie fibers suggest their strong potential for use in sustainable textile production and high-strength bio-composite applications.

Keywords: AP1 ramie fibers, alkaline–oxidative treatment, Box-Behnken Design (BBD), Response Surface Methodology (RSM), tensile strength, bio-composites

INTRODUCTION

In recent years, natural fibers have garnered significant attention as reinforcements in biocomposites due to their renewability, biodegradability, low cost, and eco-friendliness.[1-3] Among these, ramie stands out for its high cellulose content, superior tensile strength, low density, and better mechanical performance compared to other lignocellulosic fibers.[4-6] However, raw ramie fibers inherently contain substantial amounts of non-cellulosic components – such as hemicelluloses, lignin, pectin, and waxes – that hinder interfacial bonding with hydrophobic polymer matrices, ultimately limiting their performance in high-strength composites.[7-9]

To address these limitations, chemical surface modifications have been extensively explored. Alkaline treatment, predominantly with NaOH (and $Ca(OH)_2$ also explored), effectively removes amorphous constituents, enhances cellulose exposure, increases surface roughness, and improves matrix compatibility.[4,7,9] Furthermore, oxidative agents, such as hydrogen peroxide (H_2O_2), can facilitate delignification and hemicellulose cleavage via alkaline-peroxide chemistry, improving morphology, crystallinity, and interfacial behavior of treated fibers,[10-12] with numerous demonstrations in textile/pulp processes.[13-15] This combined alkaline–oxidative strategy offers a promising pathway for the production of high-performance green composites.

Characterization techniques, such as scanning electron microscopy (SEM), Fourier-transform infrared spectroscopy (FTIR), and thermogravimetric analysis (TGA), are frequently utilized to evaluate fiber transformation after treatment. SEM images typically reveal removal

of surface impurities and exposure of finer cellulose fibrils.[4,16] FTIR spectra demonstrate attenuation of hemicellulose- and lignin-associated bands (*e.g.*, C=O near ~1730 cm^{-1}; C–O–C ~1240–1260 cm^{-1}; aromatic ~1500–1600 cm^{-1}), confirming the removal of non-cellulosic phases.[8,15,17-19] Concurrently, TGA commonly shows an increase in T_{onset}/T_{max} and shifts in DTG peaks after treatment; residual char may decrease due to lignin removal, while thermal stability in the main pyrolysis region improves.[20-22]

Beyond qualitative improvements, process optimization is essential to maximize fiber performance. Parameters, such as chemical concentration, treatment time, pH, and temperature, directly influence fiber structure and function. In this regard, Response Surface Methodology (RSM) and Box–Behnken Design (BBD) have emerged as robust tools for multi-variable process optimization, allowing efficient experimental planning and accurate prediction of mechanical and chemical outcomes.[24] These techniques have been effectively applied to various natural fibers, leading to enhancements in crystallinity, surface cleanliness, and fiber–matrix interfacial strength.[25-30]

However, despite its technical potential, research on the synergistic effect of alkaline–oxidative treatments specifically applied to AP1 ramie fibers – a widely cultivated variety in Vietnam – remains limited.[31] Moreover, many existing protocols rely on prolonged durations (≈3–4 h) and high temperatures (≈90–100 °C), which challenge scalability and energy efficiency.[13,14,16] Recent studies suggest one-step alkali–H_2O_2 routes that aim to reduce temperature and time, indicating a path toward greener processing.[10,32,33]

Therefore, this study aims to develop and optimize a low-temperature oxidative–alkaline treatment for AP1 ramie fibers using $Ca(OH)_2$ and H_2O_2, targeting reductions in treatment time and chemical load, while maximizing fiber purity and strength. The influence of chemical concentration and treatment duration on morphological, chemical, thermal, and mechanical properties of the fibers was systematically evaluated using SEM, FTIR, and TGA (with FTIR assignments and crystallinity analysis guided by previously published studies).[8,17,18,34] In parallel, BBD–RSM was employed to identify optimal conditions.[24,27,28] This approach aligns with sustainable material engineering and supports circular-economy-oriented biocomposite production, mindful of environmental burdens in bleaching/dyeing industries.[12]

EXPERIMENTAL

Materials

Raw AP1 ramie fibers (*Boehmeria nivea*) were collected from the Bo Bun sub-area, Nong Truong town, Moc Chau district, Son La province, Vietnam. The main chemicals used in the oxidative–alkaline treatments included: analytical-grade calcium hydroxide ($Ca(OH)_2$, Vietnam), hydrogen peroxide (H_2O_2, 50% w/v, China), calcium hypochlorite ($Ca(OCl)_2$, 99.95% purity, China), and sodium hypochlorite solution (NaClO, 12% w/v, Vietnam). Other reagents, such as sulfuric acid (H_2SO_4, 98%, Vietnam), were used for chemical composition analysis. All reagents were of analytical grade and used without further purification.

Treatment method of AP1 ramie fibers

Prior to chemical treatment, the AP1 ramie fibers were combed, manually separated, and oven-dried at 80 °C for 2 hours to remove residual moisture. The alkaline bath was prepared by dispersing $Ca(OH)_2$ to 7 wt% (bath-mass basis) in deionized water under magnetic stirring for 15 min at 25 ± 2 °C. Immediately before fiber immersion, the oxidant was added dropwise over 2–3 min to the target level (H_2O_2 = 4 wt% from 50% stock, NaOCl = 4 wt% from a 12% solution, or $Ca(OCl)_2$ = 4 wt% as solid). After treatment under varying conditions, fibers were thoroughly washed with distilled water until neutral pH (pH = 7) and dried again at 80 °C to constant weight.

The experimental samples were denoted as shown in Table 1, and the overall processing workflow is depicted in Figure 1.

Major components in AP1 ramie samples

Determination of hemicellulose concentration[25,40]

In the first step, 1–2 grams of dried AP1 ramie fibers were weighed into 150 mL of boiled water and stored at 100 °C for 2 hours. Then, the AP1 ramie samples were filtered, washed, and dried at 105 °C to constant weight, and the recorded value was m_1. In the next step, the dried samples were put into the condenser with 150 mL of 1M H_2SO_4, and boiled at 100 °C for 1 hour. The fibers were again filtered and washed with distilled water 2–3 times, then dried at 105 °C to constant weight, and the obtained value was m_2. The hemicellulose concentration was determined by the formula (1):

$$\%\ \text{hemicelluloses} = \frac{m_1 - m_2}{m_0} * 100\% \quad (1)$$

Determination of cellulose concentration[25,40]

After determining the value of m_2 (in hemicellulose concentration assessment), the samples were further soaked in 10 mL of H_2SO_4 (72%) solution for 4 hours. Then, the samples were introduced into 150 mL of 1M H_2SO_4 solution and refluxed at 100 °C for 2 hours.

Then, the samples were filtered, washed, and dried at 105 °C in the oven. The recorded value was denoted as m_3. The cellulose concentration was determined by the formula (2):

$$\% \text{ cellulose} = \frac{m_2 - m_3}{m_0} * 100\% \quad (2)$$

Determination of lignin concentration[25,40]

After determining the value of m_3, the sample was calcined at 600 °C for 4-6 hours, then the obtained ash was weighed and the obtained mass was denoted m_4. The lignin concentration was determined using the formula (3):

$$\% \text{ lignin} = \frac{m_3 - m_4}{m_0} * 100\% \quad (3)$$

Experimental design for optimization

To optimize the oxidative–alkaline treatment of AP1 ramie fibers, a Box–Behnken design (BBD), a widely used form of Response Surface Methodology (RSM), was employed.[24,39] The three independent variables selected for the design were: calcium hydroxide concentration (A, %, w/v), treatment time (B, min), and hydrogen peroxide concentration (C, %, v/v). These variables have been shown to strongly influence the removal of lignin and hemicelluloses, the crystallinity index, and the mechanical properties of cellulose-based natural fibers.[4,9,40]

BBD was chosen for its proven efficiency in modeling quadratic responses, minimizing the number of required experimental runs, and avoiding extreme operating conditions.[24] This approach has been successfully implemented in prior optimization studies involving various lignocellulosic materials, such as banana stem, cassava bagasse, and wheat husk, demonstrating its robustness in capturing nonlinear interactions and optimizing multiple performance responses.[27,28,39]

Table 1
Sample codes and primary treatment conditions AP1

Code	Treatment route	$Ca(OH)_2$ (wt%, bath)	Oxidant (wt%, bath)	Solid-to-liquid ratio (w/v)	Temperature (°C)	Time (min)
AP1	Untreated AP1 ramie fibers	–	–	–	25 ± 2	–
AP10	Alkaline only	7	–	1:50	25 ± 2	120
AP1H	Alkaline + H_2O_2	7	H_2O_2 = 4	1:50	25 ± 2	120
AP1C	Alkaline + $Ca(OCl)_2$	7	$Ca(OCl)_2$ = 4	1:50	25 ± 2	120
AP1N	Alkaline + NaOCl	7	NaOCl = 4	1:50	25 ± 2	120

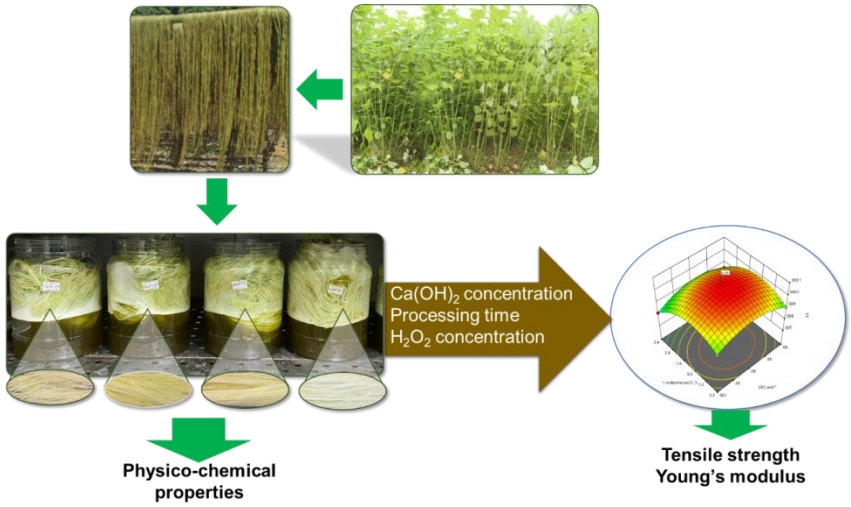

Figure 1: Illustrative diagram of the experimental

Table 2
Independent variables and their coded levels used in the Box–Behnken experimental design

Independent variables	Symbol	Coded levels		
		Low (-1)	Medium (0)	High (+1)
Calcium hydroxide concentration (%)	A	6.5	7.0	7.5
Treatment time (min)	B	80	90	100
Hydrogen peroxide concentration (%)	C	3.5	4.0	4.5

Regression modeling, the analysis of variance (ANOVA), and three-dimensional response surface plots were performed using Design Expert V23.1.0. The resulting polynomial models were used to predict fiber performance under different treatment combinations and to determine the optimal processing conditions.[24,28]

Characterization of AP1 ramie samples

The Fourier-transform infrared (FTIR) spectra of the AP1 ramie fibers were recorded using a Nicolet iS10 spectrometer (Thermo Scientific, USA) in the range of 4000–400 cm^{-1}, with a resolution of 8 cm^{-1} and 16 scans per sample. The samples were prepared in pellet form by mixing with KBr.

The surface morphology of the treated and untreated fibers was examined using field emission scanning electron microscopy (FESEM) on a JSM–6510LV microscope (JEOL, Japan) at magnifications ranging from 5× to 300,000×.

The thermal stability of the fibers was evaluated by thermogravimetric analysis (TGA) using a TG209F1 instrument (NETZSCH, Germany). Measurements were conducted from 20 °C to 600 °C, at a heating rate of 10 °C/min, under nitrogen atmosphere (flow rate: 10 cm^3/min).

The crystalline structure and nanoscale dimensions of cellulose in treated and untreated AP1 fibers were examined by X-ray diffraction (XRD) using a Bruker D8 Advance diffractometer in θ–2θ geometry over 2θ = 5–70°. Analysis focused on the positions and relative intensities of diffraction peaks to elucidate crystalline structure. The crystallinity index (CrI) was quantified from the XRD patterns based on the positions and intensities of the characteristic peaks.

The mechanical properties, including tensile strength (MPa), elongation at break (%), and Young's modulus (GPa), were measured using a Zwick Z2.5 tensile tester according to ASTM D3822, with a crosshead speed of 5 mm/min.

RESULTS AND DISCUSSION

Investigating the influence of treatment method

Weight loss, cellulose, lignin concentration, and mechanical properties of AP1 ramie fibers

The impact of oxidative–alkaline treatments on the chemical composition and mechanical behavior of AP1 ramie fibers is summarized in Table 3. All fiber samples were immersed in a 7% $Ca(OH)_2$ solution at ambient temperature for 1 hour, with or without additional oxidizing agents (H_2O_2, $Ca(OCl)_2$, NaOCl).

The untreated AP1 fibers had a cellulose content of 64.96% and a lignin content of 9.57%, with a tensile strength of 687.26 MPa. Following treatment with $Ca(OH)_2$ alone (AP10), modest improvements were observed in both cellulose content and tensile strength, attributed to the removal of amorphous hemicelluloses and partial delignification via alkali-induced swelling and disruption of hydrogen bonding. This is consistent with prior studies indicating that alkaline treatment enhances the accessibility of cellulose fibrils by removing non-cellulosic components and increasing fibril alignment.[4,9,22,40]

A markedly greater enhancement was observed with alkaline hydrogen peroxide (AP1H) treatment, which increased the cellulose content to 96.03% and reduced lignin to 1.38%. The tensile strength reached 1061.60 MPa, and Young's modulus rose to 89.35 GPa – the highest among all samples. These improvements result from the generation of reactive oxygen species (ROS), including hydroxyl radicals (•OH) and perhydroxyl anions (HOO^-), via the alkaline decomposition of H_2O_2. These ROS selectively cleave lignin ether bonds and oxidize aromatic structures, leading to solubilization of low-molecular-weight fragments and facilitating delignification and cellulose purification.[10-12]

The underlying chemistry of lignin oxidation by alkaline hydrogen peroxide involves oxidative cleavage of conjugated carbonyl structures and β–aryl ether bonds, as detailed by Gellerstedt and Agnemo.[11] These reactions disrupt the lignin macromolecule, enhancing the accessibility and crystallinity of the cellulose matrix. Treatment with hypochlorite-based oxidants (AP1C and AP1N) also significantly reduced lignin (1.54% and 1.47%, respectively) and increased cellulose content, though the mechanical properties were inferior to those of AP1H. This could be due to the non-specific and more aggressive oxidative nature of hypochlorite ions (ClO^-), which may lead to oxidative cleavage of β-1,4-glycosidic bonds in cellulose chains, resulting in structural degradation.[13,15]

Overall, the oxidative treatments can be ranked by efficiency as follows: H_2O_2 > $Ca(OCl)_2$ > NaOCl > $Ca(OH)_2$ > no treatment. Hydrogen peroxide was found to be the most effective and fiber-preserving oxidant, enabling selective delignification, while enhancing the mechanical performance of AP1 fibers for high-strength biocomposite applications.

FTIR spectra of AP1 ramie samples before and after treatment with different oxidants

Fourier-transform infrared (FTIR) spectroscopy was conducted to investigate the

structural changes in AP1 ramie fibers subjected to different oxidative–alkaline treatments. Figure 2 presents the FTIR spectra of untreated fibers (AP1), alkali-treated fibers (AP10), and those treated with combined systems, including hydrogen peroxide (AP1H), calcium hypochlorite (AP1C), and sodium hypochlorite (AP1N), all in 7% $Ca(OH)_2$ medium.

A broad band between 3000–3500 cm^{-1}, assigned to O–H stretching vibrations of hydroxyl groups in cellulose and hemicelluloses, showed a pronounced decrease after treatment, especially in the AP1H sample. This reduction reflects the disruption of hydrogen bonding networks and partial removal of hemicelluloses and lignin.[8,17,18,22,40]

The C–H stretching vibrations at 2853 and 2940 cm^{-1}, characteristic of aliphatic CH_2 groups in cellulose, remained largely unchanged across all samples, indicating that the main cellulose backbone was structurally preserved.[8,17,18]

Table 3
Weight reduction, cellulose and lignin content, and mechanical properties of AP1 ramie fibers after alkaline and oxidative treatments

Samples	Change in mass (%)	Cellulose concentration (%)	Lignin concentration (%)	Tensile strength (MPa)	Elongation at break (%)	Young's modulus, EY (GPa)
AP1	0.00	64.96	9.57	687.26 ± 4.19	1.21 ± 0.02	43.21 ± 1.10
AP10	10.78	76.08	5.78	706.15 ± 6.43	1.26 ± 0.01	52.12 ± 0.88
AP1H	26.53	96.03	1.38	1061.6 ± 5.95	1.36 ± 0.03	89.35 ± 1.60
AP1C	30.07	95.12	1.54	830.10 ± 4.23	1.31 ± 0.01	80.12 ± 1.22
AP1N	31.83	93.33	1.47	784.60 ± 6.09	1.29 ± 0.03	78.58 ± 0.98

The most significant shift occurred at 1734 cm^{-1}, corresponding to the C=O stretching of hemicelluloses and pectin ester bonds. This peak nearly disappeared in AP1H and decreased markedly in AP1C and AP1N, confirming effective hemicellulose removal – most prominently via alkaline hydrogen peroxide treatment.[8,15,17-19]

Lignin-associated aromatic skeletal vibrations at 1544 and 1517 cm^{-1} diminished substantially or vanished in the oxidant-treated samples, particularly in AP1H, indicating advanced delignification. These changes are attributable to the action of reactive oxygen species (ROS), such as hydroxyl radicals (•OH) and perhydroxyl anions (HOO^-), which selectively cleave aryl ether linkages and oxidize aromatic rings in lignin.[8,10,12,15]

The peak at 1231 cm^{-1}, corresponding to C–O stretching in aryl–alkyl ethers of lignin, also decreased significantly after oxidative treatments, supporting the above interpretation.[8,15,19]

In contrast, the peaks at 1423 cm^{-1} (CH_2 bending) and 1202 cm^{-1} (C–O–C stretching of glycosidic linkages) became more intense after treatment, especially in AP1H. This reflects enhanced exposure of crystalline cellulose domains and increased microfibrillar alignment, consistent with increased crystallinity.[17-19,33]

Overall, the spectral data clearly indicate that alkaline hydrogen peroxide treatment (AP1H) is most effective in selectively removing amorphous non-cellulosic components, while preserving and enhancing cellulose structure. The oxidation mechanism involves ROS-mediated cleavage of β–aryl ether and carbonyl-conjugated structures in lignin, as thoroughly described by Gierer.[12]

XRD patterns and crystallinity

XRD (Cu Kα) confirms the cellulose-I allomorph for all samples, with reflections at ≈15–16.5° ((1–10)/(110)), 22.6° ((200)), and 34.5° (004).[22,37,40] Representative diffractograms are shown in Figure 3, where the cellulose-I reflections are indexed and the untreated *vs*. treated patterns are directly compared. Relative to alkali treatment alone (AP1), the peroxide-assisted alkaline route (AP1H) yields a sharper (200) peak (FWHM(200): 2.285° → 2.074°) and a weaker amorphous halo near ≈18°, indicating improved lattice ordering.[4,27,34] Consistently, the Scherrer crystallite size for (200) increases slightly (D(200): 3.71 → 4.09 nm).[4,27,37]

Using the Segal peak-height method, the crystallinity indices are CrI_{AP1} = 88.98% and

CrI_{AP1H} = 86.76%. The modest decrease for AP1H is attributable to a higher/amplified I_{am} located near ~19.28° and a slightly elevated amorphous background, underscoring the method sensitivity of Segal CI to baseline selection and preferred orientation.[27,34,36] As emphasized in recent methodology reviews, Segal CI is prone to over-/under-estimation when the amorphous contribution is not properly isolated; peak-fitting/amorphous-subtraction or Rietveld approaches typically yield different (often lower) absolute CI values and are better used for relative trends within a consistent dataset.[27,33,36] Accordingly, despite the slightly lower Segal CI, the narrower FWHM and larger D(200) indicate greater lattice ordering in AP1H; after baseline correction or peak deconvolution, CI would be expected to align with this trend.[34,36] In line with observations on enzyme- or peroxide-assisted treatments, improvements in lattice order do not always translate into higher Segal CI if the analysis relies solely on the (200) peak and an uncorrected amorphous background.[27,33] No cellulose-II reflections (~12.1°/20.1°) are detected, confirming preservation of cellulose-I under the mild, room-temperature treatment.[22,37,38] The increased structural order (lower FWHM, larger D(200)) together with the high CI values is consistent with the observed gains in tensile strength and modulus, supporting the mechanism that selective removal of non-cellulosics enhances the load-bearing cellulose domains.[7,21,37]

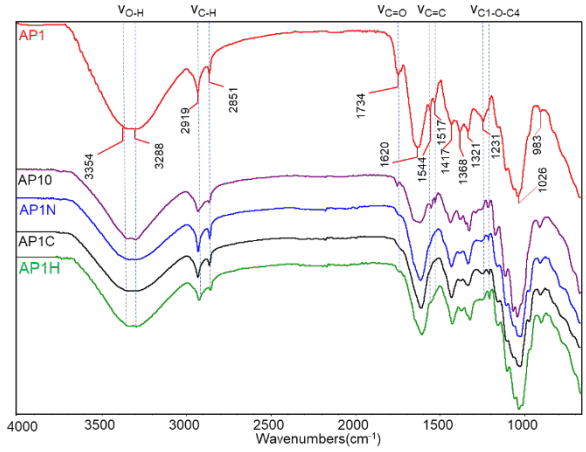

Figure 2: FTIR spectra of AP1 ramie fiber samples AP1, AP1H, AP1C, AP1N, AP10

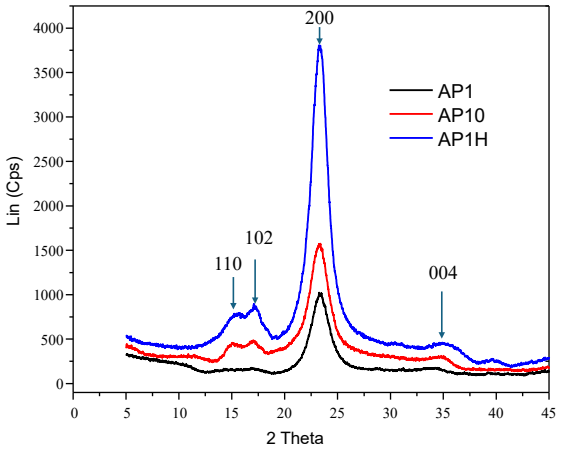

Figure 3: XRD patterns of AP1, AP1.0 and AP1H

SEM images of AP1 ramie samples

The surface morphology and microstructural transformations of AP1 ramie fibers subjected to different chemical treatments were examined using scanning electron microscopy (SEM), as illustrated in Figure 4.

The untreated fibers (AP1, Fig. 4a) exhibited densely packed bundles with irregular, coarse surfaces covered by waxy, lignin-rich, and hemicellulose-derived residues. These impurities hinder interfacial bonding and stress transfer in composite matrices. Similar observations were reported in raw kenaf and date palm fibers, where residual surface deposits contributed to poor mechanical performance in composites.[9,29]

After treatment with 7% $Ca(OH)_2$ alone (AP10, Fig. 4b), minor surface smoothing and partial defibrillation occurred, but most non-cellulosic components remained. This outcome aligns with Modibbo *et al.*,[37] who showed that mercerization or mild alkaline treatments without oxidative agents fail to sufficiently disrupt the lignin–hemicellulose complex. The incomplete surface refinement confirms that alkaline treatment alone is inadequate for high-purity fiber preparation.

In the samples treated with NaOCl (AP1N, Fig. 4c) and $Ca(OCl)_2$ (AP1C, Fig. 4d), more noticeable fiber separation and removal of surface coatings were observed. However, residual irregularities and fibril agglomerations were still present. According to the textile-bleaching literature,[13,15] oxidants with lower redox selectivity, such as hypochlorites, are less effective for selective lignin cleavage and often require longer reaction times or elevated temperatures for substantial purification. Moreover, hypochlorites can induce partial oxidative degradation of cellulose, compromising the uniformity of surface cleaning.

The most significant morphological transformation occurred in the AP1H sample (Fig. 4e), treated with hydrogen peroxide in alkaline medium. The surface was smooth, clean, and free of impurities, with clear microfibrillar separation and a more aligned structure. This can be attributed to the formation of hydroxyl radicals (•OH) under alkaline H_2O_2 conditions, which selectively cleave β-O-4 ether and aromatic linkages in lignin, while leaving cellulose relatively untouched.[11,12] Rafidison *et al.*[19] also observed similarly refined and clean surfaces in fibers treated by oxidative–alkaline systems, demonstrating superior delignification and hemicellulose removal.

SEM-based fiber diameter analysis (Fig. 4, right column) confirmed a progressive decrease in mean fiber diameter from 64 µm (AP1) to 37 µm (AP1H), along with a narrower and more symmetric diameter distribution in AP1H. This implies uniform defibrillation and better exposure of microfibrils. Such morphological improvement is crucial for enhancing fiber–matrix adhesion in composite applications. Edeerozey *et al.*[9] reported that NaOH-treated kenaf fibers with cleaner surfaces and narrower diameter distributions led to better tensile performance. Similarly, Taha *et al.*[29] emphasized that surface uniformity and fibril separation are strong indicators of optimized fiber–resin interaction.

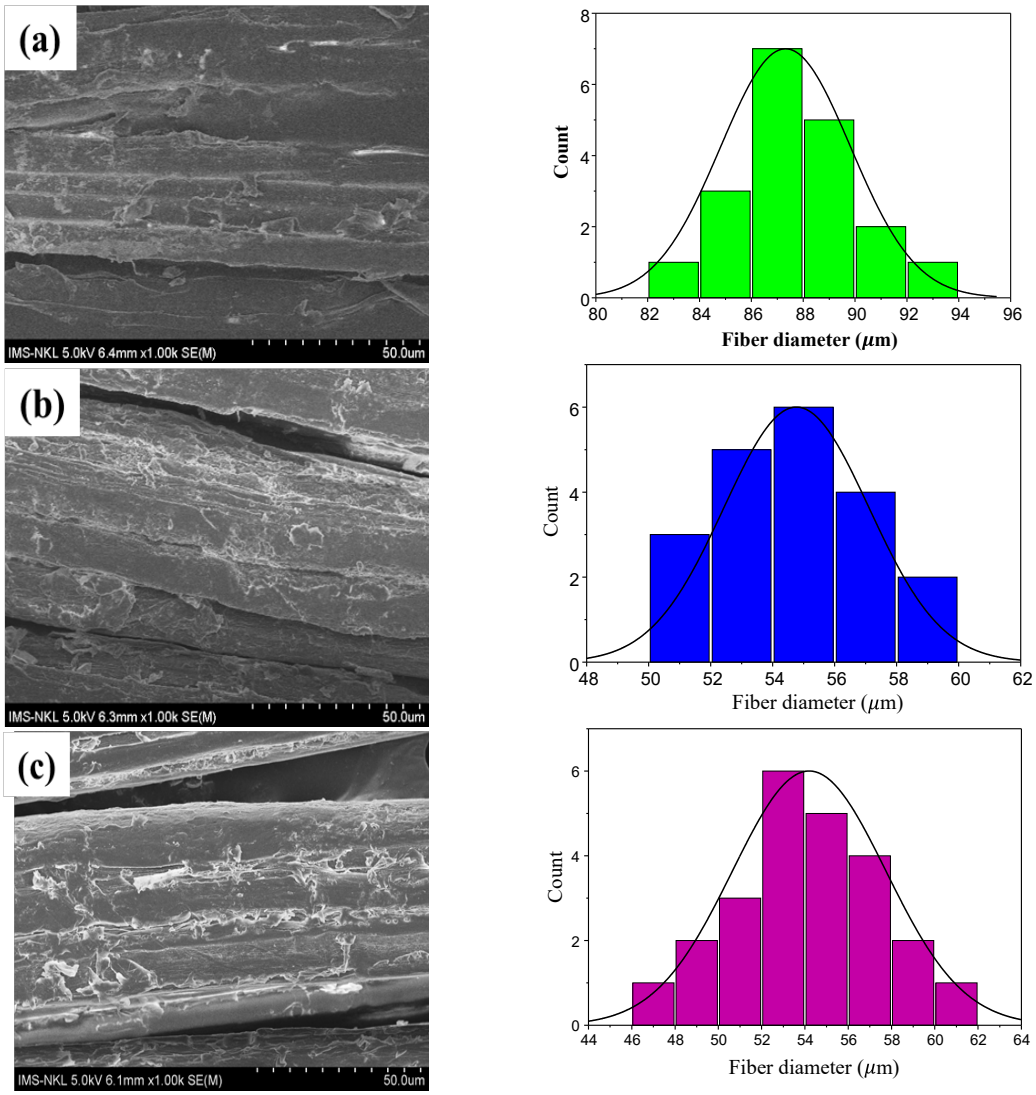

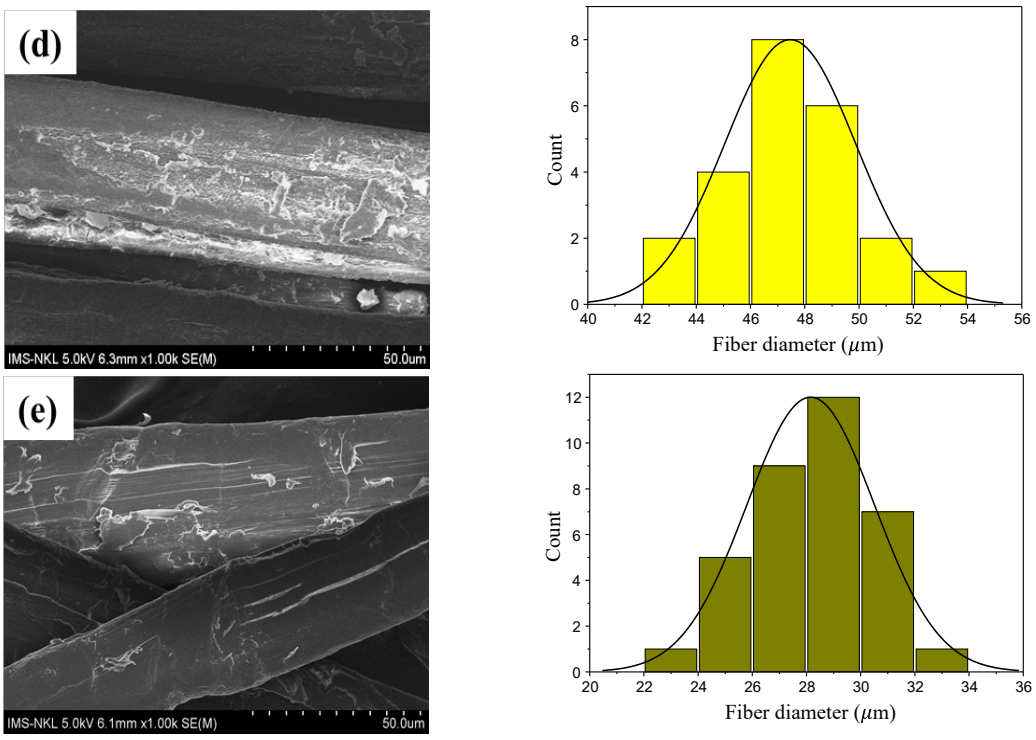

Figure 4: SEM images of AP1 ramie treated with different oxidants AP1 (a), AP10 (b), AP1N (c), AP1C (d), AP1H (e) – with all treatments conducted for 120 min at room temperature

Further validation comes from Zhang *et al*.,[43] who investigated copper ammonia-treated ramie fabrics and observed a reduction in fiber diameter from 35.8 µm to 24.6 µm after controlled treatment. Their SEM images revealed that reduced diameter was associated with less prickle and improved softness. These findings are in agreement with the present AP1H results, where smaller and more regular fibers suggest superior process selectivity and structural refinement.

What is particularly noteworthy is that the optimized AP1H process achieved these effects under mild conditions – room temperature and only 1.5 hour of treatment. This is in contrast to traditional bleaching or alkali treatments that often require temperatures above 90 °C for extended durations (3–4 hours) to induce similar morphological changes.[13,14] The environmental and energy-saving advantages of the H_2O_2–$Ca(OH)_2$ system further highlight its viability for sustainable composite production.

In summary, SEM analysis reveals that, among the studied treatments, the AP1H protocol yields the most structurally refined ramie fibers. The high level of surface purity, microfibrillar separation, and diameter reduction observed in AP1H can be attributed to the selective delignification and hemicellulose removal facilitated by hydroxyl radicals. This morphological improvement provides a strong foundation for the mechanical enhancement of AP1 fibers when used in advanced biocomposite materials.

Effects of the treatment method on the properties of ramie AP1 fibers

The thermal behavior of untreated (AP1) and alkaline hydrogen peroxide-treated (AP1H) ramie fibers was investigated by thermogravimetric analysis (TGA) and derivative thermogravimetry (dTG), as presented in Figure 5 and summarized in Table 4. Both samples exhibited a typical three-step decomposition pattern characteristic of lignocellulosic fibers, in agreement with previous studies on ramie, hemp, and banana fibers.[20,22,40]

In the first decomposition stage (30–120 °C), the observed weight loss was associated with the evaporation of adsorbed moisture. The AP1 fibers exhibited higher moisture loss (7.6%) compared to AP1H (4.1%), indicating that the oxidative–alkaline treatment reduced hygroscopicity by effectively removing hemicelluloses and pectin. This observation is consistent with findings from Nguyen Thi Thuy Van[42] and Liu *et al*.,[32] who reported reduced moisture retention in peroxide-treated banana fibers and in urea–H_2O_2-treated lignocellulosic fibers.

The second stage (200–300 °C) corresponds to the thermal decomposition of hemicelluloses and low-molecular-weight pectins. AP1 fibers exhibited a mass loss of 13.9%, while AP1H lost only 5.4%, confirming the selective removal of thermally labile components via hydrogen peroxide oxidation under alkaline conditions. Similar reductions in hemicellulose-derived weight loss have been reported in alkali–peroxide-treated ramie and *Helicteres isora* fibers.[22,31,38,40]

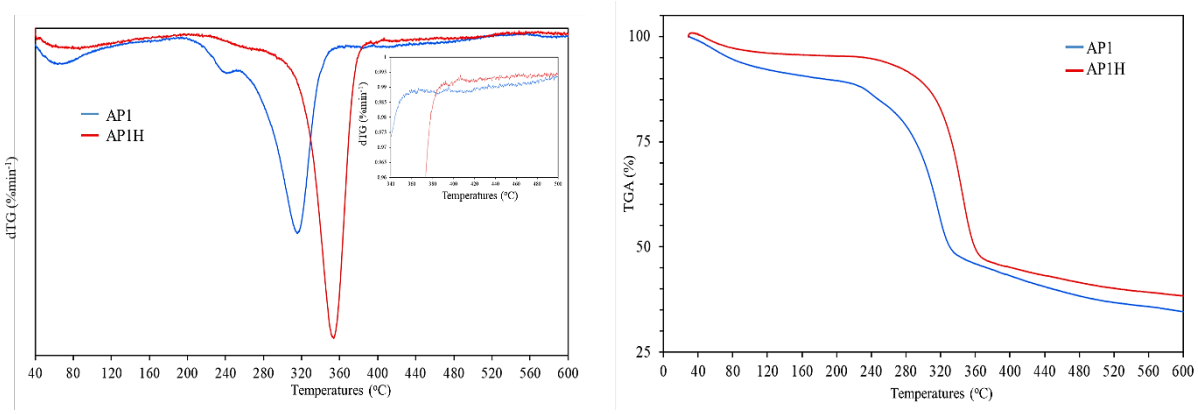

Figure 5: DTG and TGA diagrams of AP1 and AP1H ramie fibers

Table 4
Thermal degradation characteristics of AP1 and AP1H ramie fibers

Temperature of decomposition stages (°C)	Maximum temperature (°C)		Mass reduction (%)		Remaining mass at 600 °C (%)	
	AP1	AP1H	AP1	AP1H	AP1	AP1H
30 – 120	64	76	7.6	4.1	34.6	38.3
200 – 300	241	279	13.9	5.4		
300 – 380	315	354	39.8	46.4		
380 – 600	383	399	55.7	54.8		

In the third stage (300-600 °C), corresponding to the degradation of cellulose and residual lignin, the AP1H fibers showed a notably higher degradation peak temperature (354 °C) compared to AP1 (315 °C), indicating enhanced thermal stability. This improvement is attributed to increased cellulose purity and possible condensation of oxidized lignin fragments.[10-12] The greater residual mass at 600 °C (38.3% in AP1H vs. 34.6% in AP1) supports the formation of a more thermally resilient carbonaceous framework, consistent with observations on alkali/oxidatively treated kenaf and Sansevieria fibers.[9,40]

The dTG profiles revealed a sharper and right-shifted peak for AP1H, reflecting delayed degradation onset and improved structural order. These trends are characteristic of cellulose-rich materials with minimal amorphous content.[20,22,40]

The underlying mechanism can be attributed to the generation of reactive oxygen species (ROS), particularly hydroxyl radicals (•OH) and superoxide anions (O_2^-), during H_2O_2 decomposition in alkaline medium. Under controlled alkaline–peroxide conditions, these radicals preferentially attack lignin and hemicelluloses, while largely preserving cellulose, as detailed by More[10] and by the classic peroxide-chemistry analyses of Gellerstedt and Agnemo,[11] and Gierer.[12] Consequently, oxidative–alkaline treatment improves thermal integrity by eliminating unstable components while stabilizing the cellulose matrix.

Notably, these thermal enhancements were achieved under mild processing conditions (room temperature, 1.5 hour), as opposed to conventional methods requiring elevated temperatures and prolonged durations. The improved thermal profile of AP1H confirms the potential of this rapid and environmentally friendly method for thermally stable, bio-based composite applications.[13,14,31]

Effects of H_2O_2 concentration

Following the identification of hydrogen peroxide (H_2O_2) as the most effective oxidizing agent, a series of experiments was conducted to investigate the influence of varying H_2O_2 concentrations (1–5 wt% based on fiber weight) on the treatment efficiency of AP1 ramie fibers. The corresponding samples were denoted as AP1H1%, AP1H2%, AP1H3%, AP1H4%, and AP1H5%, as shown in Table 5.

Weight loss and cellulose content trends are illustrated in Figure 6. With increasing H_2O_2 concentration, both parameters showed a positive trend: cellulose content improved from 80.5% at 1% H_2O_2 to 94.7% at 5%. This behavior reflects the progressive removal of hemicelluloses and lignin by oxidative delignification, as similarly reported in previous studies on ramie and bast fibers.[16,31,32] These results confirm the efficacy of the alkaline H_2O_2 system in fiber purification and compositional refinement.

Tensile strength results (Fig. 7) indicated a gradual increase up to 4% H_2O_2 (1054.4 MPa), followed by a slight reduction at 5% (998.2 MPa). This observation suggests that excessive peroxide induces over-oxidation, generating elevated levels of reactive species (•OH, O_2•$^-$) that may non-selectively attack cellulose chains and initiate depolymerization. Hydroxyl-radical reactions under excessive alkaline-peroxide conditions can cause cellulose chain scission – cleaving β-1,4-glycosidic linkages – and thereby reduce the degree of polymerization and fiber integrity.[10-12]

Table 5
Sample codes for AP1 ramie fibers treated with different H_2O_2 concentrations

Sample	Symbols
AP1 ramie fibers treated with 1% H_2O_2	AP1H1%
AP1 ramie fibers treated with 2% H_2O_2	AP1H2%
AP1 ramie fibers treated with 3% H_2O_2	AP1H3%
AP1 ramie fibers treated with 4% H_2O_2	AP1H4%
AP1 ramie fibers treated with 5% H_2O_2	AP1H5%

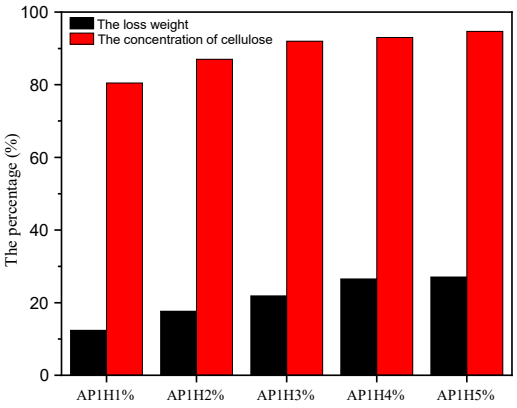

Figure 6: Weight loss and concentration of cellulose in different samples

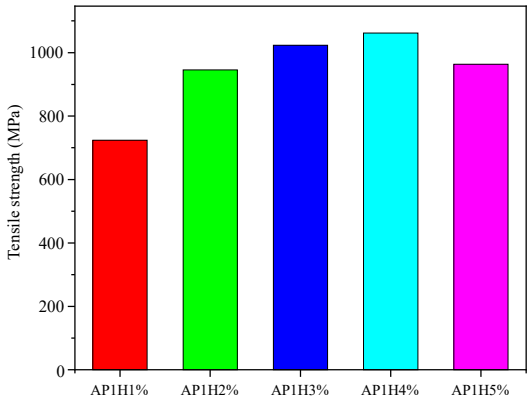

Figure 7: Tensile strength of different samples

FTIR analysis (Fig. 8) substantiates these findings. The progressive attenuation of the ~1734 cm^{-1} band (assigned to C=O stretching in hemicellulose/pectin esters) and concurrent increase in C–O–C band intensity (1032–1060 cm^{-1}) signal the effective removal of non-cellulosic components and an increase in cellulose order. These spectral trends mirror those observed in peroxide-treated jute and kenaf fibers, where the loss of ester and lignin-related peaks corresponds with compositional purification.[8,15,17,18,19]

Quantitative FTIR analysis (Fig. 8) shows a monotonic decrease of hemicellulose/lignin markers up to 4% H_2O_2, followed by a plateau or slight reversal at 5%, consistent with incipient cellulose oxidation at higher peroxide loadings. The aliphatic C–H stretching band at ~2919 cm^{-1} – well separated from adjacent absorptions – was used as the internal reference.[17,18] Relative

concentration indices (RCI) were determined as follows:

$$RCI_{C=O}(x\%) = \frac{\left[\frac{D_{1734}}{D_{2919}}\right]_{x\%}}{\left[\frac{D_{1734}}{D_{2919}}\right]_{0}} \quad (4)$$

$$RCI_{C\text{-}O\text{-}C}(x\%) = \frac{\left[\frac{D_{1203}}{D_{2919}}\right]_{x\%}}{\left[\frac{D_{1203}}{D_{2919}}\right]_{0}} \quad (5)$$

where D_i is the integrated absorbance of band *i*; subscript x% denotes fibers treated at H_2O_2 concentration x% for 120 min, and 0 denotes the untreated control. Band assignments: 1734 cm^{-1} (C=O of hemicellulose/pectin esters) and ~1202–1203 cm^{-1} (C–O–C, β-1,4-glycosidic).[8,15,17,18,19] The observed levelling or slight decrease of the cellulose-associated index at 5% H_2O_2 agrees with tensile data (Fig. 9) and with reports that excessive alkaline-peroxide can induce cellulose chain scission in amorphous domains.[10-12]

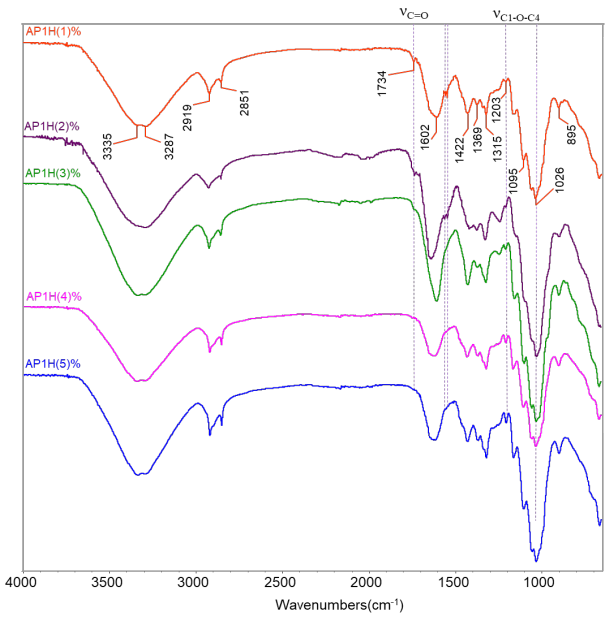

Figure 8: FTIR spectra of AP1 ramie fibers after treatment with H_2O_2 in different concentrations (from 1% to 5%)

Quantitative changes in FTIR absorbance (Fig. 8) reinforce this trend. Decreases in lignin/hemicellulose bands, together with a rise in cellulose-associated bands, point to enhanced cellulose content up to 4% H_2O_2. However, at 5%, spectral intensity plateaus or even declines slightly, implying potential cellulose chain degradation. This correlates with tensile strength data and prior observations by Gellerstedt and Agnemo,[10,11] who noted that excessive H_2O_2 leads to unwanted oxidation of cellulose amorphous regions.

The reaction mechanism is illustrated schematically in Figure 10. Under alkaline conditions, H_2O_2 decomposes into highly reactive hydroxyl (•OH) and superoxide ($O_2^{\bullet-}$) radicals, which preferentially cleave β-O-4 ether bonds in lignin and ester bonds in hemicelluloses. However, when radical concentration becomes too high – as at ≥5% H_2O_2 – the amorphous zones in cellulose become susceptible to attack, resulting in depolymerization and fiber weakening.[10-12,33]

Colorimetric analysis (Fig. 11) also supports the trend. The ΔE values, indicative of fiber whitening, increased with peroxide concentration up to 4%, then plateaued at 5%. This result mirrors the chromophore removal behavior observed in ramie fibers treated via Fenton and other oxidative systems.[13,16] Meanwhile, scanning electron microscopy (data not shown) revealed increased fibrillation and microvoid formation at 5%, consistent with over-oxidation-induced surface degradation.

Taken together, these results suggest that a 4% H_2O_2 concentration in combination with 7% $Ca(OH)_2$ provides the optimal balance between fiber purification and structural integrity. Beyond this threshold, the marginal gains in cellulose content are offset by loss in mechanical properties due to cellulose degradation. Thus, 4% H_2O_2 appears ideal for enhancing fiber performance, while minimizing damage – aligning with prior

optimization studies on oxidative degumming systems.[16,31,32]

Effects of time on the properties of ramie AP1 fibers under optimum treatment conditions

The influence of treatment duration on the physicochemical and mechanical properties of AP1 ramie fibers was systematically investigated under the optimized alkaline–oxidative conditions, namely 7% calcium hydroxide ($Ca(OH)_2$) and 4% hydrogen peroxide (H_2O_2). The corresponding results are illustrated in Figure 12.

As shown, fiber weight loss increased rapidly during the initial 5 minutes of treatment, reaching approximately 21.4%, and then gradually rose to 32.1% at 90 minutes. This trend indicates a time-dependent dissolution of amorphous constituents, such as pectin, hemicelluloses, waxes, and loosely bound lignin.

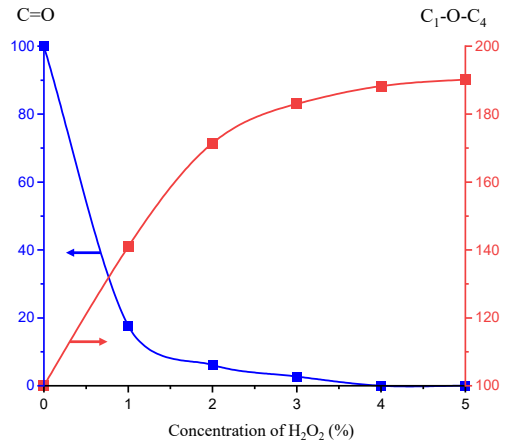

Figure 9: Effect of H_2O_2 concentration on conversion efficiency of C=O, C_1-O-C_4 functional groups in AP1 ramie fibers during processing

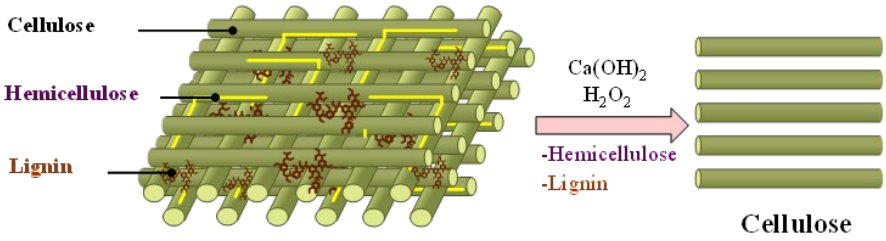

Figure 10: Schematic representation of delignification and hemicellulose removal in AP1 ramie fibers treated with a $Ca(OH)_2$ and H_2O_2 system

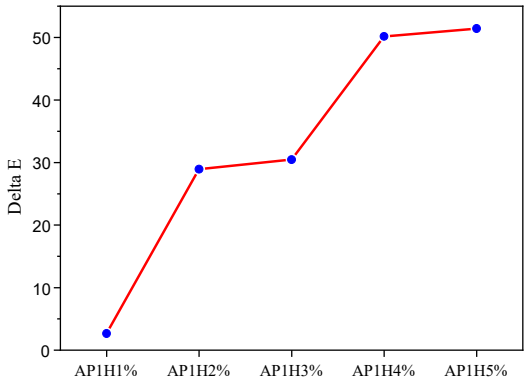

Figure 11: Effects of H_2O_2 concentration on colour changes of AP1 ramie fibers

The alkaline environment facilitates fiber swelling and enhances peroxide penetration, thereby accelerating delignification and hemicellulose breakdown.[4,9,16] Similar behavior has been observed in other lignocellulosic systems, where increasing treatment time enhanced purification, but also elevated the risk of fiber degradation.[16,31,32,40]

Simultaneously, the tensile strength improved markedly from 687.3 MPa (untreated) to a maximum of 1061.6 MPa after 90 minutes, corresponding to the effective removal of non-cellulosic fractions and exposure of highly ordered cellulose regions. These structural refinements – confirmed by prior SEM and FTIR analyses – promote microfibrillar alignment and facilitate stress transfer at the fiber–matrix interface.[4,9,16] The tensile performance enhancement is also consistent with previous studies reporting similar effects in peroxide-treated bast fibers.[16,31,32,40]

However, extending the treatment to 120 minutes resulted in a slight decline in tensile strength (to 962.9 MPa), which is likely attributed to excessive oxidative exposure. Under prolonged alkaline–peroxide conditions, hydroxyl (•OH) and superoxide ($O_2^{\bullet -}$) radicals generated from H_2O_2 decomposition may begin to cleave β-1,4-glycosidic bonds within amorphous cellulose regions, leading to chain scission, microvoid formation, and structural weakening.[10-12] This phenomenon has been previously reported in over-delignified fibers where the oxidation exceeded the critical threshold for cellulose preservation.[16,22,31,32]

These findings highlight that a treatment duration of 90 minutes with the current system offers an optimal balance between component removal and structural retention. Extending beyond this duration yields diminishing returns in compositional purity and compromises mechanical integrity. Therefore, time optimization is essential for maximizing the performance of AP1 fibers in high-strength composite applications.

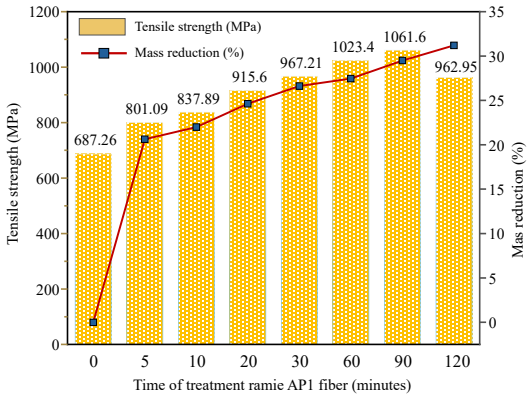

Figure 12: Effects of processing time of AP1 ramie fibers on weight loss and tensile strength

Optimization of AP1 ramie fiber processing

Experimental results of optimization

To determine the optimal processing conditions for AP1 ramie fibers, a three-factor, three-level Box-Behnken Design (BBD) was implemented using Response Surface Methodology (RSM) in Design Expert version 23.1.0.[24,39] The independent variables were calcium hydroxide concentration (A, %, w/v), treatment time (B, minutes), and hydrogen peroxide concentration (C, %, v/v), while the two selected response variables were tensile strength (Y_1, MPa) and Young's modulus (Y_2, GPa). The full experimental matrix is presented in Table 6, and the statistical significance of each factor and interaction is summarized in Table 7.[7,24,28]

Table 6 shows that tensile strength (Y_1) and modulus (Y_2) varied considerably with the experimental conditions. The highest tensile strengths – 1061.6 and 1062.15 MPa – were obtained at the center points (A = 7.0%, B = 90 min, C = 4.0%), confirming that moderate alkali/oxidant levels with sufficient time give optimal reinforcement. This trend aligns with prior reports on alkaline treatment windows for bast fibers, including flax/ramie systems.[22,39]

The significance of the quadratic regression equation model of the AP1 ramie fibers

processing and the coefficients were assessed through ANOVA analysis, with the results shown in Table 7.

Table 6
Experimental matrix and results of the objective function values

Run	$Ca(OH)_2$ concentration (%, A)	Time (min, B)	H_2O_2 concentration (%, C)	Y_1	Y_2
1	7.0	80	3.5	903.71 ± 6.27	77.02 ± 1.52
2	6.5	90	4.5	974.34 ± 4.33	76.83 ± 1.10
3	7.5	90	3.5	894.75 ± 3.87	75.42 ± 0.82
4	7.0	100	4.5	810.74 ± 4.06	72.61 ± 1.89
5	7.0	90	4.0	1061.6 ± 5.95	89.35 ± 1.60
6	7.5	90	4.5	713.01 ± 4.48	66.93 ± 1.11
7	6.5	80	4.0	1024.2 ± 3.00	67.35 ± 0.84
8	7.0	90	4.0	1059.42 ± 6.26	89.75 ± 0.72
9	7.0	100	3.5	911.94 ± 3.12	84.83 ± 1.52
10	7.0	80	4.5	853.67 ± 3.81	83.12 ± 1.16
11	7.5	80	4.0	816.85 ± 3.15	73.77 ± 1.47
12	6.5	100	4.0	965.97 ± 3.71	79.15 ± 1.73
13	7.5	100	4.0	844.85 ± 4.68	60.75 ± 2.11
14	6.5	90	3.5	953.17 ± 4.57	73.72 ± 1.75
15	7.0	90	4	1062.15 ± 3.75	90.14 ± 1.73

Table 7
ANOVA data for the reactions

Source	Objective function			
	Y_1		Y_2	
	F – value	P – value	F – value	P – value
Model	3141.19	< 0.0001	118.95	< 0.0001
A	9707.62	< 0.0001	52.25	0.0008
B	97.40	0.0002	1.97	0.2192
C	2246.20	< 0.0001	16.97	0.0092
AB	343.57	< 0.0001	158.08	< 0.0001
AC	1902.41	< 0.0001	34.53	0.0020
BC	120.94	0.0001	86.12	0.0002
A^2	3076.53	< 0.0001	594.16	< 0.0001
B^2	4471.41	< 0.0001	152.86	< 0.0001
C^2	8271.75	< 0.0001	43.32	0.0012
Lack of Fit	3.66	0.2220	4.55	0.1855
R^2	0.9998		0.9978	
R^2 correction	0.9995		0.9937	
Adeq. Precision	183.2175		50.3296	

The ANOVA data in Table 7 confirm model significance for both responses (Y_1: F = 3141.19, $p < 0.0001$; Y_2: F = 118.95, $p < 0.0001$). Among main effects, A ($Ca(OH)_2$) and C (H_2O_2) showed the strongest influences ($p < 0.0001$) on both responses. B (time) significantly affected tensile strength ($p = 0.0002$), but not modulus ($p = 0.2192$), suggesting tensile strength is more sensitive to reaction kinetics than stiffness – consistent with observations on ramie/plant fibers under alkaline–oxidative conditioning.[4,28]

Interaction terms (AB, AC, BC) were also highly significant ($p < 0.0001$), underscoring parameter synergy; notably, AC (alkali × peroxide) exerted a pronounced effect, in line with reports emphasizing oxidative–alkaline balance in fiber refinement.[31,32] Significant quadratic terms (A^2, B^2, C^2) further confirm non-linearity and the need for response-surface optimization.[24,28]

Model robustness is supported by high R^2 (0.9998 for Y_1; 0.9978 for Y_2) and adjusted R^2 (0.9995; 0.9937), with Adeq. Precision values of

183.22 and 50.33, indicating strong signal-to-noise and predictive capability.[24,28]

Notably, similar optimization outcomes have been reported for natural fibers: date-palm alkali optimization via RSM,[29] bast-fiber systems with peroxide/alkali windows,[31] and oxidative degumming of ramie where moderate oxidant doses outperformed extremes due to structural preservation[16] – all corroborating the present optimum of A = 7.0%, B = 90 min, C = 4.0% as a favorable balance between delignification, integrity, and mechanical enhancement.

Overall, the quadratic regression models developed here are statistically significant and predictive, consistent with validated RSM methodologies for fiber-treatment optimization.[24,28,29,39]

Assessment of significance of the model

The statistical performance of the second-order regression model, constructed using the Box–Behnken design (BBD), was evaluated based on the analysis of variance (ANOVA) results presented in Table 6. The model exhibited exceptional predictive strength, with F-values of 3141.19 for tensile strength (Y_1) and 118.95 for Young's modulus (Y_2), both associated with p-values below 0.0001, confirming the overall significance of the model terms.[24,28]

The coefficients of determination (R^2) were 0.9998 for Y_1 and 0.9978 for Y_2, indicating that the models explained over 99% of the variation in the responses. The adjusted R^2 values (0.9995 for Y_1 and 0.9937 for Y_2) further corroborated the robustness of the models by accounting for the number of predictors. In addition, the adequate precision ratios – 183.22 for tensile strength and 50.33 for modulus – greatly exceeded the minimum threshold value of 4, highlighting excellent signal-to-noise ratios within the design space.[24,28] These findings are consistent with earlier optimization studies on flax,[39] ramie[4] and composite fibers,[29] which emphasize the reliability of RSM-derived models for predicting fiber behavior.

The parity plots in Figure 13 demonstrate a strong correlation between experimental and predicted values, with data points tightly clustered along the 45° diagonal. The residuals were randomly distributed within ±6.25 units, suggesting a lack of systematic error and confirming the accuracy and lack of bias in the model.

After removing statistically insignificant variables ($p > 0.05$), the final second-order regression equations were derived as follows:

$$Y_1 = 1061.6 - 81.03A - 8.12B - 38.98C + 21.56AB - 50.73AC - 12.79BC - 67.14A^2 - 80.95B^2 - 110.10C^2 \quad (1)$$

$$Y_2 = 89.75 - 2.52A - 0.49B - 1.44C - 6.20AB - 2.9AC - 4.58BC - 12.83A^2 - 6.66B^2 - 3.69C^2 \quad (2)$$

The regression coefficients revealed that all linear terms (A, B, and C) exerted negative effects on the responses, indicating that excessive levels of individual variables can reduce tensile strength and stiffness. This reflects the concept of an optimum in response surface methodology, beyond which further increases in process parameters lead to deterioration in fiber structure and properties.[4,24,28,31]

All interaction terms (AB, AC and BC) were found to be statistically significant ($p < 0.001$), underscoring the importance of synergistic effects among process variables. Notably, the AC interaction (alkali–oxidant) had the strongest influence on tensile strength, supporting observations from Widodo,[40] who emphasized the critical role of oxidative–alkaline balance in fiber refinement. For Young's modulus, the interaction term AB and the quadratic effect A^2 were particularly influential, suggesting that fiber stiffness is more sensitive to the interplay between alkali strength and reaction time, which concurs with the findings.[4,28] These results are consistent with previous studies employing RSM for fiber optimization. Aly *et al*.[39] observed a decline in tensile strength of flax fibers when alkali concentrations exceeded the optimal level. Similarly, studies on banana fibers have reported signs of cellulose damage under oxidative/alkaline treatments, consistent with over-oxidation effects at higher peroxide loadings.[31,32,42] Zhou *et al*.[16] found that oxidative degumming of ramie using Fenton reagents achieved superior mechanical properties at moderate oxidant levels, highlighting the importance of dosage control.[16]

In conclusion, the BBD-based regression models developed in this study are statistically robust, highly predictive, and scientifically sound. They effectively capture the non-linear and interactive effects of treatment variables and provide a reliable foundation for optimizing AP1 ramie fiber processing in sustainable high-performance composite applications.[24,28,29,39]

Analyzing the influence of technological parameters on the objective function Y_1

The interactive effects of technological parameters – namely $Ca(OH)_2$ concentration (A), treatment time (B), and H_2O_2 concentration (C) – on the mechanical properties of AP1 ramie fibers were thoroughly examined using three-dimensional response surface plots and their corresponding contour diagrams (Fig. 14 for Y_1, Fig. 15 for Y_2). These visualizations offer valuable insight into the nonlinear behavior and synergistic interactions between processing variables.

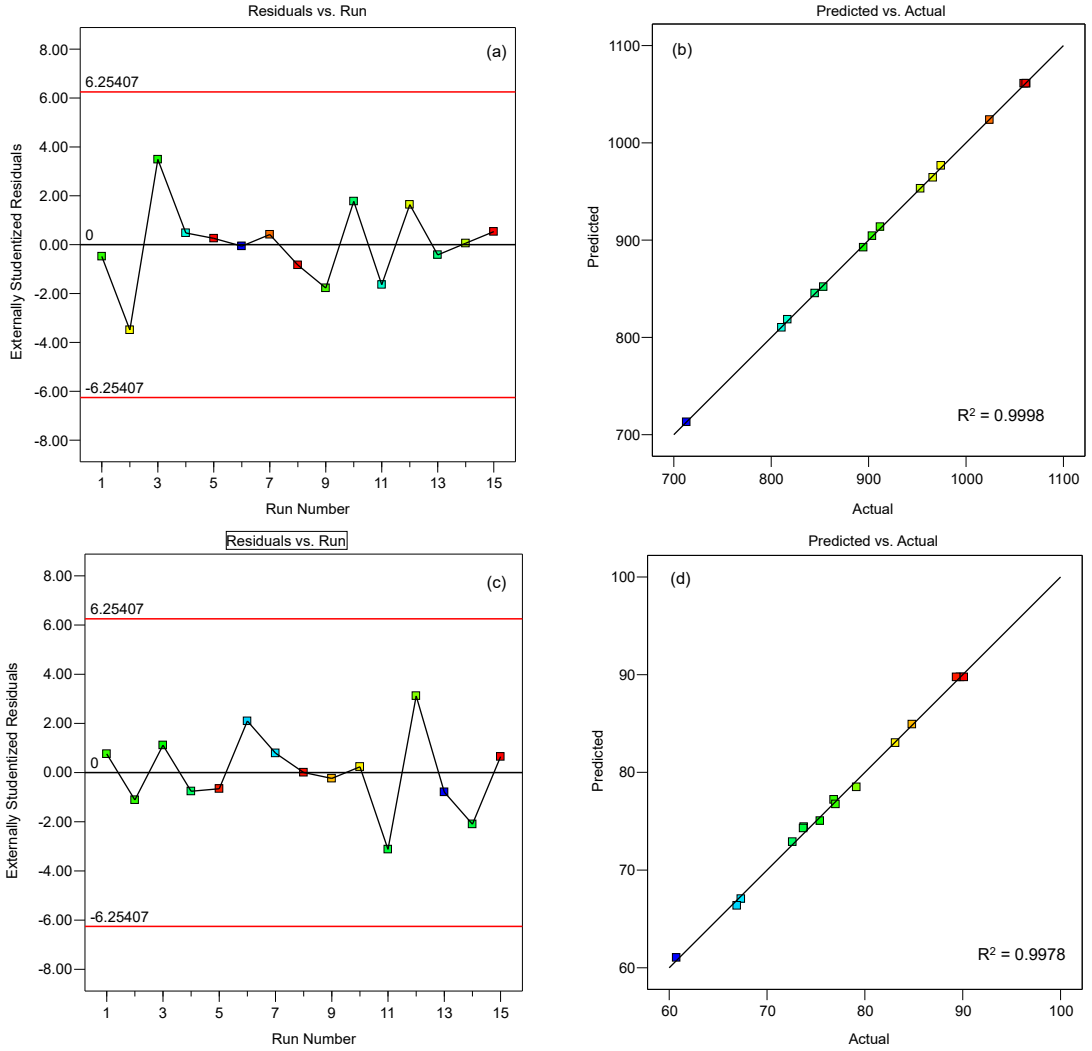

Figure 13: Graphs for experimental and predicted values, random distribution of Y_1, Y_2

As shown in Figure 14a, increasing both $Ca(OH)_2$ concentration and treatment time initially enhances tensile strength, likely due to the progressive removal of amorphous matrix components – primarily hemicelluloses and surface lignin – which in turn exposes and aligns crystalline cellulose microfibrils. However, beyond a threshold (A > 7.0% and B > 90 minutes), tensile strength begins to decline, suggesting partial degradation of cellulose chains under extended alkaline–oxidative exposure. This trend is consistent with previous studies reporting mechanical deterioration caused by β-1,4-glycosidic bond cleavage when alkali or processing time is excessive.[10-12,31]

Figure 14b illustrates the interaction between $Ca(OH)_2$ and H_2O_2 concentrations. An optimal region is evident at intermediate levels of both reagents, while higher peroxide concentrations (> 4%) reduce tensile strength due to intensified depolymerization of cellulose. This behavior aligns with the observations of Widodo[40] and

Zhou *et al.*,[16] who emphasized that oxidative damage beyond a critical oxidant threshold leads to chain scission and fiber embrittlement. In Figure 14c, the interaction between treatment time and H_2O_2 concentration further highlights the sensitivity of the fiber system to over-oxidation. Prolonged exposure at high peroxide levels promotes excessive delignification and degradation of structural polysaccharides, leading to a measurable reduction in tensile strength beyond 90 minutes. This is supported by prior studies, which reported that over-processing during peroxide bleaching caused microstructural damage and mechanical weakening in natural fibers.[13,14,16]

The optimal region – centred around A = 7.0%, B = 90 minutes, and C = 4.0% – corresponds to a peak tensile strength of approximately 1062 MPa. This validates the predictive accuracy of the response surface model and is in close agreement with prior optimization studies on banana and ramie fibers. Studies on banana fibers reported signs of cellulose damage under oxidative/alkaline treatments, consistent with over-oxidation at higher peroxide loadings.[42] Meanwhile, Zhou *et al.*[16] confirmed that moderate oxidant dosages in Fenton-based degumming of ramie yielded superior mechanical properties compared to more aggressive treatments.

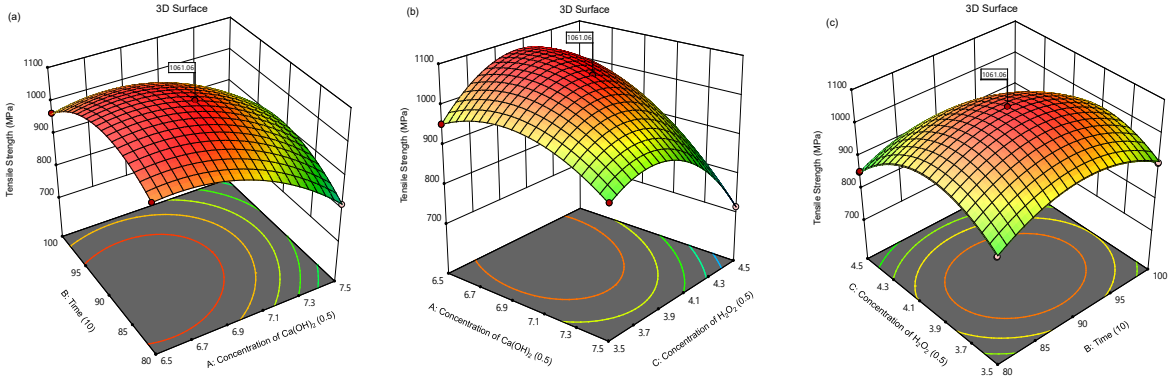

Figure 14: Response surface plots of technological factor pairs on the target function Y_1

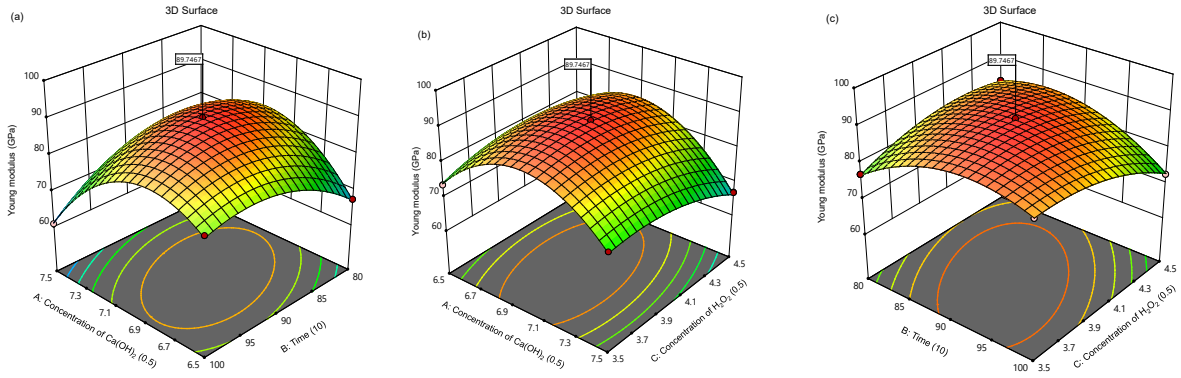

Figure 15: Response surface plots of technological factor pairs on the target function Y_2

Turning to Young's modulus (Y_2), the corresponding plots (Fig. 15) indicate that stiffness is more sensitive to chemical concentrations than to treatment time. Figure 15a reveals a pronounced nonlinear relationship between $Ca(OH)_2$ concentration and modulus, with a maximum at ~7.0%, followed by a decline attributed to microvoid formation and cellulose matrix disruption.[4,39] Figures 15b and 15c show that H_2O_2-related interactions (with time and alkali) exhibit parabolic trends: moderate oxidative levels enhance fiber stiffness by exposing crystalline domains, while excessive conditions lead to modulus reduction due to over-fragmentation, as also noted in prior studies.[29,39,45]

Statistical analysis in Table 6 reinforces these empirical findings. All interaction terms (AB, AC, BC) were statistically significant ($p < 0.001$), confirming that fiber mechanics are governed by

nonlinear, synergistic effects among chemical concentration and treatment duration.[24,28]

In conclusion, the response surface and contour analyses clearly demonstrate that moderate levels of $Ca(OH)_2$ and H_2O_2, combined with a treatment time of 90 minutes, provide the most favorable conditions for optimizing tensile strength and stiffness in AP1 ramie fibers. The consistency between model predictions, experimental data, and prior literature[4,16,22,31,32,39] affirms the validity and applicability of the optimization strategy for sustainable bio-composite applications.

Optimization of AP1 ramie fiber processing conditions and validation testing

The optimal processing conditions for AP1 ramie fibers were identified using the desirability function approach integrated in Design Expert version 23.1.0.[24,28] This multi-objective optimization technique aimed to simultaneously maximize tensile strength (Y_1) and Young's modulus (Y_2). Among 100 generated solutions, the second-ranked solution achieved the highest global desirability value (1.000), corresponding to the processing condition of 7.0% $Ca(OH)_2$ concentration, 90 minutes of treatment time, and 4.0% H_2O_2 concentration (Fig. 16).

Under these optimized conditions, the model predicted tensile strength and Young's modulus values of 1061.6 MPa and 89.35 GPa, respectively. These values reflect a favorable balance between efficient delignification and preservation of cellulose microstructure. The performance improvement is attributed to synergistic effects between alkali-induced fiber swelling, oxidative cleavage of hemicellulose and lignin linkages, and enhanced microfibrillar alignment – mechanisms previously documented in optimized fiber systems.[4,16,36]

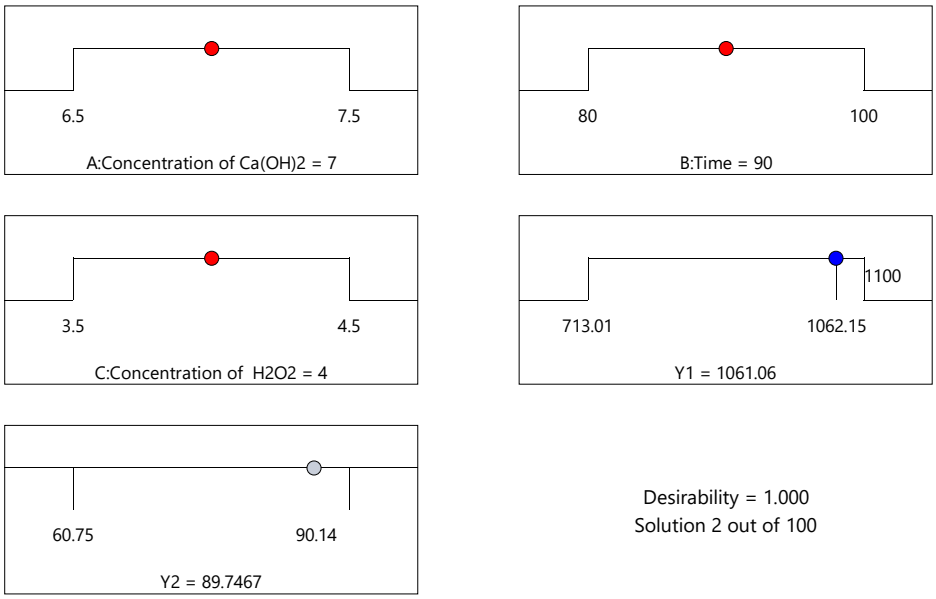

Figure 16: Optimal conditions and predicted values of the target functions Y_1 and Y_2

Table 8
Confirmation test results with optimized AP1 ramie fibers processing parameters

$Ca(OH)_2$ conc. (%)	Time (min)	H_2O_2 conc. (%)	Tensile strength (%)		Young's modulus (GPa)		Error (%)	
			Predicted	Actual	Predicted	Actual	Tensile strength	Young's modulus (MPa)
7	90	4	1061.6	1083.5 ± 4.13	89.35	91.42 ± 1.77	2.06	2.32

To validate the model predictions, triplicate confirmation experiments were performed under the identified optimal conditions. The measured tensile strength and modulus were 1083.5 ± 4.13 MPa and 91.42 ± 1.77 MPa, respectively. These results deviated by only 2.06% and 2.32% from

the predicted values (Table 8), confirming the high predictive accuracy and reliability of the developed RSM-based model.[24,28,39]

These findings are in strong agreement with prior studies. Studies on banana fibers reported improvements under moderate oxidative–alkaline conditions;[42] in alkaline–peroxide systems, higher peroxide loadings can induce cellulose oxidation and performance loss.[10-12,31,32] Similarly, Zhou *et al*.[16] reported that Fenton-based oxidative degumming of ramie achieved optimal mechanical outcomes when oxidant levels were maintained within a controlled range. Prior studies have demonstrated that excessive oxidative exposure during peroxide bleaching can lead to fibrillar disruption and loss of mechanical strength.[13,14,16]

Furthermore, the use of the desirability function has been widely validated in natural fiber processing as an effective tool for solving multi-objective optimization problems. Aly *et al*.[39] employed this technique to successfully optimize chemical treatments in flax fibers, achieving a close match between model predictions and experimental results. Similarly, Yaro *et al*.[30] and Aly *et al*.[39] applied desirability analysisto composite optimization, confirming its robustness for balancing multiple performance criteria.

A concise benchmarking shows that optimally treated AP1 ramie fibers (≈1061.6 MPa; ≈89.35 GPa; ≈1.36%) sit at the very top end of bast fibers: their tensile strength clearly exceeds typical hemp (≈550–900 MPa) and jute (≈393–800 MPa) and is within the upper band reported for flax (≈345–1500 MPa). Meanwhile, AP1's Young's modulus (~89 GPa) surpasses the usual ranges for flax (27–80 GPa), hemp (38–70 GPa), and jute (10–30 GPa), while elongation remains in the characteristic 1–3% window of bast fibers.[7,20] Taken together, AP1 provides a best-in-class stiffness–strength profile among common natural fibers, making it a strong candidate for high-performance biocomposites; as usual, cross-study comparisons may vary with gauge length, humidity, and test standards, but the overall advantage remains clear.[7,20]

In summary, the integration of Box–Behnken design, response surface modeling, and desirability function analysis produced a statistically robust and practically scalable optimization framework. The validated optimal condition (7.0% $Ca(OH)_2$, 90 minutes, 4.0% H_2O_2) yielded AP1 ramie fibers with outstanding mechanical properties, making them highly suitable for sustainable, high-performance biocomposite applications.

The exploratory NaOCl and $Ca(OCl)_2$ arms were included as controls to benchmark the proposed alkaline–peroxide route.[13] While hypochlorites are technically effective oxidants, their use can raise sustainability concerns due to potential formation of adsorbable organic halides (AOX) and chlorinated by-products in effluents.[13,14] In bench-scale trials, alkaline pH (≥10) was maintained to suppress chlorination side-reactions and residual active chlorine was quenched with sodium thiosulfate prior to neutralization and waste collection.[13,14] By contrast, the $Ca(OH)_2$–H_2O_2 pathway does not generate AOX and is therefore more aligned with best-practice guidance for low-impact pretreatment.[13,14] Accordingly, hypochlorite-assisted treatments are positioned as comparative controls only and are not recommended for scale-up in applications targeting greener processing.[13,14]

CONCLUSION

In this study, an environmentally friendly oxidative–alkaline treatment process for AP1 ramie fibers was successfully developed and systematically optimized. The findings demonstrated that alkaline treatment using 7% $Ca(OH)_2$ alone resulted in limited delignification and insufficient mechanical enhancement (untreated fibers: cellulose 64.96%, lignin 9.57%, tensile strength 687.26 MPa), whereas incorporating hydrogen peroxide (H_2O_2) as an oxidant markedly improved treatment efficiency by enabling deeper penetration and more selective degradation of non-cellulosic components.

The optimal treatment condition – 7.0% $Ca(OH)_2$ and 4.0% H_2O_2 for 90 minutes – was identified using response surface methodology (RSM) and experimentally validated with <3% deviation between predicted and measured responses. Under these conditions, the treated AP1 fibers exhibited a cellulose content of 96.03%, tensile strength of 1061.60 MPa (a 54.4% increase compared to untreated fibers), Young's modulus of 89.35 GPa, and a reduced average fiber diameter of 37 μm. Thermogravimetric analysis further indicated selective removal of thermally labile fractions (second-stage hemicellulose-related weight loss reduced to ≈ 5.4%) and a higher residual mass at 600 °C (38.3% in AP1H vs. 34.6% in AP1), while FTIR and XRD showed attenuation of

lignin/hemicellulose bands and modest lattice ordering gains (*e.g*., D(200): 3.71 → 4.09 nm), consistent with effective delignification, microfibrillar exposure, and enhanced crystallinity.

The regression models developed using RSM and desirability analysis exhibited strong predictive accuracy, confirmed by R^2 = 0.9998 (tensile) and 0.9978 (modulus), very high adequate-precision ratios (183.22 for tensile; 50.33 for modulus), and parity plots with residuals distributed within ±6.25 units, indicating no systematic bias. The main effects of $Ca(OH)_2$ and H_2O_2 were highly significant ($p < 0.0001$), treatment time affected tensile strength ($p = 0.0002$), and interaction terms AB, AC, BC were statistically significant, with AC (alkali–oxidant) particularly influential – consistent with the curvature observed in the response surfaces and the identified optimum.

Importantly, this study provides a robust and scalable framework for processing natural fibers under mild conditions – room temperature, 90-min residence, and reduced chemical consumption – thereby minimizing energy input and secondary pollution. The optimized AP1 fibers are well-suited for high-performance, biodegradable composites, with potential applications in sustainable packaging, automotive interiors, and eco-friendly construction materials. Overall, the proposed oxidative–alkaline method offers a promising alternative to conventional harsh chemical treatments, combining operational simplicity, environmental compatibility (no AOX formation for the peroxide route), and superior material quality, thereby contributing to green manufacturing aligned with circular-economy and carbon-neutral goals.

REFERENCES

[1] D. Romanzini, H. L. Ornaghi Junior, S. C. Amico and A. J. Zattera, *Mat. Res.*, **15**, 415 (2012), https://doi.org/https://doi.org/10.1590/S1516-14392012005000050

[2] M. Saha, H. Singh, M. K. Singh, S. M. Rangappa and S. Siengchin, *Sustain. Chem. Climate Act.*, **6**, 100081 (2025), https://doi.org/10.1016/j.scca.2025.100081

[3] M. A. Akar, A. T. Tosun, F. Yel and U. Kumlu, *Macromol. Symp.*, **404**, 2100414 (2022), https://doi.org/10.1002/masy.202100414

[4] M. Cai, H. Takagi, A. N. Nakagaito, Y. Li and G. I. N. Waterhouse, *Composites A*: *Appl. Sci. Manuf.*, **90**, 589 (2016), https://doi.org/10.1016/j.compositesa.2016.08.025

[5] S. Shahinur, M. Hasan, Q. Ahsan, N. Sultana, Z. Ahmed *et al*., *Polymers*, **13**, 2571 (2021), https://doi.org/10.3390/polym13152571

[6] W. Lv, K. Nie, Y. Song, C. Li, H. Ben *et al*., *J. Nat. Fibers*, **19**, 3681 (2022), https://doi.org/10.1080/15440478.2020.1848719

[7] M. M. Kabir, H. Wang, K. T. Lau and F. Cardona, *Appl. Surface Sci.*, **276**, 13 (2013), https://doi.org/10.1016/j.apsusc.2013.02.086

[8] K. P. Sao, M. D. Mathew and P. K. Ray, *Text. Res. J.*, **57**, 407 (1987), https://doi.org/10.1177/004051758705700706

[9] J. Gierer, in *Procs. Symposium on Wood and Pulping Chemistry*, Helsinki, Finland, June 6-8, 1995, vol. I, pp. 285-291

[10] A. More, T. Elder and Z. Jiang, *Holzforschung*, **75**, 806 (2021), https://doi.org/10.1515/hf-2020-0165

[11] G. Gellerstedt, R. Agnemo, J. Dale, K. Daasvatn, J.-E. Berg *et al*., *Acta Chem. Scand.*, **34b**, 275 (1980), https://doi.org/10.3891/acta.chem.scand.34b-0275

[12] A. Hashem and S. Farag, *Int. J. Adv. Manuf. Technol.*, (2025), https://doi.org/10.1007/s00170-025-16185-4

[13] F. Wang, Y.-B. Zheng, X.-X. Cao, Z.-Q. Du and J.-J. Long, *Arab. J. Chem.*, **17**, 105953 (2024), https://doi.org/10.1016/j.arabjc.2024.105953

[14] A. K. Roy, S. C. Bag, D. Sardar and S. K. Sen, *J. Appl. Polym. Sci.*, **43**, 2187 (1991), https://doi.org/10.1002/app.1991.070431205

[15] M. D. Teli and J. M. Terega, *IRJET*, **04**, 67 (2017)

[16] C. Y. Liang and R. H. Marchessault, *J. Polym. Sci.*, **39**, 269 (1959), https://doi.org/10.1002/pol.1959.1203913521

[17] R. H. Marchessault and C. Y. Liang, *J. Polym. Sci.*, **43**, 71 (1960), https://doi.org/10.1002/pol.1960.1204314107

[18] B. H. Rafidison, H. Ramasawmy, J. Chummun and F. B. V. Florens, *SN Appl. Sci.*, **2**, 1922 (2020), https://doi.org/10.1007/s42452-020-03667-1

[19] N. Sgriccia and M. Hawley, *Compos. Sci. Technol.*, **67**, 1986 (2007), https://doi.org/10.1016/j.compscitech.2006.07.031

[20] X. Zhang, J. Yang, Y. Wang, C. Duan, Y. Liu *et al*., *J. Nat. Fibers*, **20**, 2120150 (2023), https://doi.org/10.1080/15440478.2022.2120150

[21] P. Acharya, D. Pai, K. S. Bhat and G. T. Mahesha, *J. Nat. Fibers*, **21**, 2406454 (2024), https://doi.org/10.1080/15440478.2024.2406454

[22] G. R. Mike, *IJST*, **13**, 384 (2020), https://doi.org/10.17485/ijst/2020/v13i04/147288

[23] M. A. Bezerra, R. E. Santelli, E. P. Oliveira, L. S. Villar and L. A. Escaleira, *Talanta*, **76**, 965 (2008), https://doi.org/10.1016/j.talanta.2008.05.019

[24] U. L. Jamilah and S. Sujito, *JSMI*, **22**, 62 (2021), https://doi.org/10.17146/jsmi.2021.22.3.6182

[25] D. F. Hincapié Rojas, T. R. Romero Rodriguez, D. F. Ortega Solarte, O. Moscoso Londoño, C. L. Londoño Calderón *et al*., *Cellulose Chem. Technol.*, **58**, 437 (2024),

https://doi.org/10.35812/CelluloseChemTechnol.2024.58.42
[26] W. A. Woldie, N. T. Shibeshi and K. D. Kuffi, *Carbohyd. Polym. Technol. Appl.*, **9**, 100707 (2025), https://doi.org/10.1016/j.carpta.2025.100707
[27] J. Q. A. Brito, F. D. S. Dias, S. Cunha, L. P. Ramos and L. S. G. Teixeira, *Biotechnol. Progress*, **35**, e2802 (2019), https://doi.org/10.1002/btpr.2802
[28] A. M. M. Edeerozey, H. M. Akil, A. B. Azhar and M. I. Z. Ariffin, *Mater. Lett.*, **61**, 2023 (2007), https://doi.org/10.1016/j.matlet.2006.08.006
[29] A. E. Bekele, H. G. Lemu and M. G. Jiru, *J. Compos. Sci.*, **7**, 37 (2023), https://doi.org/10.3390/jcs7010037
[30] P. Q. Tuấn, Đ. Q. Thầm, N. T. T. Trang, N. T. Thái and N. T. Hương, *Tạp Chí Phân Tích Hóa, Lý Và Sinh Học*, **26**, 141 (2021)
[31] H. Chen, Z. Wang, B. Jiang, M. Liu, H. Chen *et al.*, *BioResources*, **20**, 8791 (2025), https://doi.org/10.15376/biores.20.4.8791-8810
[32] G. L. Liu, Z. F. Li, R. Y. Ding, X. M. Zhong and C. W. Yu, *AMM*, **121-126**, 3039 (2011), https://doi.org/10.4028/www.scientific.net/AMM.121-126.3039
[33] N. S. A. Yaro, M. B. Napiah, M. H. Sutanto, A. Usman and S. M. Saeed, *Construct. Build. Mater.*, **298**, 123849 (2021), https://doi.org/10.1016/j.conbuildmat.2021.123849
[34] K. Ranganathan, S. Jeyapaul and D. C. Sharma, *Environ. Monit. Assess.*, **134**, 363 (2007), https://doi.org/10.1007/s10661-007-9628-z
[35] D. Beyene, M. Chae, J. Dai, C. Danumah, F. Tosto *et al.*, *Materials*, **11**, 1272 (2018), https://doi.org/10.3390/ma11081272
[36] L. Jing, Y. Jiang, L. Li and T. Zhang, *J. Nat. Fibers*, **20**, 2237681 (2023), https://doi.org/10.1080/15440478.2023.2237681
[37] U. U. Modibbo, B. A. Aliyu and I. I. Nkafamiya, *Int. J. Phys. Sci.*, **4**, 698 (2009)
[38] L. Cheng, S. Duan, X. Feng, K. Zheng, Q. Yang *et al.*, *J. Eng. Fibers Fabr.*, **15**, 1 (2020), https://doi.org/10.1177/1558925020940105
[39] M. Aly, M. S. J. Hashmi, A. G. Olabi, K. Y. Benyounis, M. Messeiry *et al.*, *J. Nat. Fibers*, **9**, 256 (2012), https://doi.org/10.1080/15440478.2012.738036
[40] E. Widodo, Pratikto, Sugiarto and T. D. Widodo, *Case Stud. Chem. Environ. Eng.*, **9**, 100546 (2024), https://doi.org/10.1016/j.cscee.2023.100546
[41] N. Thi Thuy Van, P. Gaspillo, H. G. T. Thanh, N. H. T. Nhi, H. N. Long *et al.*, *Heliyon*, **8**, e11845 (2022), https://doi.org/10.1016/j.heliyon.2022.e11845
[42] I. Taha, L. Steuernagel and G. Ziegmann, *Compos. Interfaces*, **14**, 669 (2007), https://doi.org/10.1163/156855407782106528
[43] J. Zhou, Z. Li and C. Yu, *Fibers Polym.*, **18**, 1891 (2017), https://doi.org/10.1007/s12221-017-6489-0
[44] H. Pratiwi, Kusmono and M. W. Wildan, *Results Eng.*, **25**, 104164 (2025), https://doi.org/10.1016/j.rineng.2025.104164